

ORIGINAL RESEARCH

10-Gingerol alleviates hypoxia/reoxygenation-induced cardiomyocyte injury through inhibition of the Wnt5a/Frizzled-2 pathway

Bin Zheng¹ | Jiaying Qi¹ | Panpan Liu¹ | Muqing Zhang¹ | Yuanyuan Zhang¹ |
Yucong Xue¹ | Xue Han¹ | Shan Xu² | Li Chu^{1,3} 

¹School of Pharmacy, Hebei University of Chinese Medicine, Shijiazhuang, China

²Affiliated Hospital, Hebei University of Chinese Medicine, Shijiazhuang, China

³Hebei Key Laboratory of Chinese Medicine Research on Cardio-cerebrovascular Disease, Shijiazhuang, China

Correspondence

Xue Han, School of Pharmacy, Hebei University of Chinese Medicine, 326 Xinshi South Road, Shijiazhuang, Hebei, China.
Email: hanxuecc@126.com

Shan Xu, Affiliated Hospital, Hebei University of Chinese Medicine, 389 Zhongshan East Road, Chang'an District, Shijiazhuang, Hebei, China.
Email: xushan20202020@163.com

Professor Li Chu, School of Pharmacy, Hebei University of Chinese Medicine, 326 Xinshi South Road, Shijiazhuang, Hebei, China.
Email: chuli0614@126.com

Funding information

Science and Technology Research Project of Hebei Province, Grant/Award Number: BJ2020002

Abstract

10-Gingerol (10-Gin), an active ingredient extracted from ginger, has been reported to have beneficial effects on the cardiovascular system. However, 10-Gin has not been proved to offer protection against cardiomyocyte injury induced by hypoxia/reoxygenation (H/R). This study aimed to investigate the protective effects of 10-Gin against H/R-induced injury and its potential mechanisms in cardiomyocytes. A H/R injury model of H9c2 cardiomyocytes was established using 600 $\mu\text{mol/L}$ CoCl_2 to induce hypoxia in the cells for 24 hr and then reoxygenated for 3 hr. 10-Gin was pretreated with H9c2 cardiomyocytes for 24 hr to assess its cardiomyocyte protection. Our results showed that 10-Gin improved the viability of H9c2 cardiomyocytes in the H/R model and decreased the activities of creatine kinase, lactate dehydrogenase, and the generation of reactive oxygen species. By intracellular Ca^{2+} ($[\text{Ca}^{2+}]_i$) fluorescence, we found that 10-Gin could significantly reduce the $[\text{Ca}^{2+}]_i$ concentration. 10-Gin administration increased the activities of antioxidant and reduced malondialdehyde content and inflammatory cytokine levels. 10-Gin also reduced the apoptosis levels. Importantly, 10-Gin administration decreased the gene and protein expressions of Wnt5a and Frizzled-2. In conclusion, 10-Gin alleviates H/R-induced cardiomyocyte injury, which is associated with the antioxidation, anti-inflammation, antiapoptosis action, and reduction of $[\text{Ca}^{2+}]_i$ overload by suppressing the Wnt5a/Frizzled-2 pathway.

KEYWORDS

10-Gingerol, H9c2 cardiomyocyte, CoCl_2 , hypoxia/reoxygenation, intracellular Ca^{2+} overload, Wnt5a/Frizzled-2 pathway

Bin Zheng, Jiaying Qi should be considered joint first author.

This is an open access article under the terms of the Creative Commons Attribution License, which permits use, distribution and reproduction in any medium, provided the original work is properly cited.

© 2021 The Authors. *Food Science & Nutrition* published by Wiley Periodicals LLC.

1 | INTRODUCTION

Cardiovascular disease is a major cause of elevated human mortality, and its incidence is increasing (Aissaoui et al., 2020). Acute myocardial infarction (AMI) is a common cardiovascular disease that endangers human health (Najib et al., 2015). Previous studies have shown that AMI has high morbidity and mortality, and myocardial ischemia/reperfusion injury (MIRI) is an important cause of this condition (Herlitz et al., 2008; Najib et al., 2015). MIRI refers to an irreversible disease in which ischemic myocardial damage is aggravated after revascularization (Yellon & Hausenloy, 1997). MIRI is associated with a series of clinical problems, including thrombolysis, angioplasty, and coronary bypass surgery (Turer & Hill, 2010). With the application of reperfusion technology in AMI treatment, MIRI caused by reperfusion has become a hot topic in cardiovascular disease research. Therefore, there is an urgent need for new treatments for AMI to prevent and alleviate MIRI.

Currently, it is believed that the main pathogenesis of MIRI is the production of oxygen free radical (OFR) and the formation of intracellular Ca^{2+} ($[\text{Ca}^{2+}]_i$) overload (Turer & Hill, 2010). The generation of OFR is an important step in the progression toward MIRI, and $[\text{Ca}^{2+}]_i$ overload is the terminal link of irreversible injury (Tani, 1990; Turer & Hill, 2010). Excess OFR can cause severe oxidative stress damage, leading to the abnormal function of the endoplasmic reticulum and $[\text{Ca}^{2+}]_i$ overload (Jennings, 2013). Moreover, inflammatory and oxidative stress are closely linked and are characteristics of cardiac diseases (Cachofeiro et al., 2008). During MIRI, oxidative stress causes endoplasmic reticulum damage and reactivation of mitochondria (Jennings, 2013). The mitochondrial membrane potential (MMP) is restored, and Ca^{2+} is driven into the mitochondria through the single transporter, and the mitochondrial permeability transition pore (mPTP) is induced to open (Weiss et al., 2003). As a result, the homeostasis of $[\text{Ca}^{2+}]_i$ is destroyed, resulting in increased Ca^{2+} influx, unbalanced free Ca^{2+} reuptake, and Ca^{2+} accumulation in the cytoplasm (Weiss et al., 2003). The significantly increased free Ca^{2+} concentration in the cytoplasm will eventually lead to cell necrosis, apoptosis, enhanced autophagy, and cell degeneration (Aldakkak et al., 2011; Eefting et al., 2004).

The Wnt/Frizzled signaling pathway is considered the regulation target of various cardiovascular diseases (Blankestijn et al., 1997). It has been proven that after myocardial infarction, the Wnt/Frizzled pathway is activated in the process of myocardial reconstruction and heart failure (Sheldahl, Park, Miller & Moon., 2000). Wnt5a is believed to be closely associated with $[\text{Ca}^{2+}]_i$ metabolism, and its activation can trigger $[\text{Ca}^{2+}]_i$ release through the Wnt/ Ca^{2+} pathway. Importantly, the above effects of Wnt5a are realized through the activation of the Frizzled-2 receptor (Slusarski and Corces et al., 1997). Furthermore, the overexpression of Frizzled-2 can activate the Wnt5a/Frizzled-2 pathway, thereby inducing the accumulation of Ca^{2+} , and this effect can be reversed by inhibiting Frizzled-2 (Zhou et al., 2012).

Ginger (*Zingiber officinale* Roscoe, *Zingiberaceae*), a perennial herb of the zingiberaceae family, is native to South Asia, and it has long been used as a daily spice flavoring around the world (Ghareib

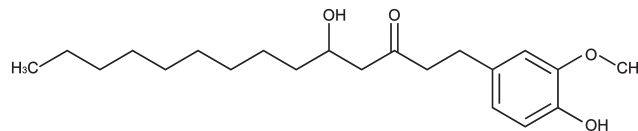


FIGURE 1 Chemical structure formula of 10-Gin

et al., 2015). People in ancient Greece, China, and India have used ginger to treat various diseases (Haniadka et al., 2012). Ginger contains a variety of phenolic components that have been shown to possess biological activities, including antioxidation, antitumor, anti-inflammatory, and antiglycemic activities (Ali et al., 2008; Bode et al., 2001; Katiyar et al., 1996; Minghetti et al., 2007; Shukla & Singh, 2007). In our previous studies, we have demonstrated that 6-Gin, a component from ginger, protects against myocardial fibrosis (Han et al., 2020) and can significantly inhibit L-type Ca^{2+} current and alleviate myocardial ischemia in vivo and in vitro (Han et al., 2019). However, 10-Gin ($\text{C}_{21}\text{H}_{34}\text{O}_4$; Figure 1), the main ingredient in gingerol and similar to 6-Gin, has not been shown to have a protective effect on MIRI, and its underlying mechanism has not been studied.

We hypothesized that 10-Gin offers protection to H9c2 cardiomyocyte injury induced by hypoxia/reoxygenation (H/R). In our study, the protection of 10-Gin was determined by detecting the viability of H9c2 cells and the levels of oxidative stress, $[\text{Ca}^{2+}]_i$ concentration, inflammation, and apoptosis in the H/R model. Furthermore, the underlying mechanisms were explored by detecting the protein and gene expression levels of the Wnt5a/Frizzled-2 pathway. Our research provides new strategies and methods for mitigating MIRI in the treatment of AMI.

2 | MATERIALS AND METHODS

2.1 | Reagents

10-Gin (Biopurify, China, Catalog: BP0013, HPLC $\geq 98\%$) was dissolved in dimethyl sulfoxide to prepare a 100 mmol/L stock solution. All kits used in this experiment were purchased from the Jiancheng Bioengineering Institute of Nanjing (Nanjing, China). High-glucose Dulbecco's modified Eagle's medium (DMEM, Catalog: 12,430,047), fetal bovine serum (FBS, Catalog: 10,093,188), trypsin (Catalog: 25,200,072), and penicillin/streptomycin were purchased from Gibco (Thermo Fisher Scientific, Inc. Missouri, USA). Unless otherwise stated, the other chemical reagents of analytical grade were obtained from Sigma-Aldrich (Missouri, USA).

2.2 | Cell culture

The rat H9c2 cardiomyoblasts (Bluebio, Shanghai, China, Catalog: BFN60804388) were cultured in high-glucose DMEM containing 10% FBS and 100 U/mL penicillin/streptomycin in 5% CO_2 and 95% air at 37 °C. The medium was changed every 2 days. The cells were digested with 0.25 g/L trypsin and counted when the degree of

cell fusion was about 80%. The cells were inoculated into a 25-cm² culture flask for passage every 3 days. H9c2 cardiomyocytes at the logarithmic growth stage were taken for subsequent experiments.

2.3 | Establishment of the H/R model

CoCl₂ (Catalog: 449,776) is a common chemical anoxic reagent that can simulate ischemic/hypoxia conditions in various cells (Jung et al., 2007). H9c2 cardiomyocytes were prepared into 5×10^4 /ml cell suspension and inoculated in a 96-well plate at 100 μ L/well. After the cells were incubated in an incubator containing 5% CO₂ at 37 °C for 24 hr, the cells were treated with hypoxia when the degree of cell fusion reached 80%–100%. CoCl₂ solutions with different concentrations (200, 400, 600, 800, and 1,000 μ mol/L) were prepared with high-glucose DMEM and incubated for 24 hr, respectively, and the optimal concentration of hypoxia was determined according to the results of cell counting kit-8 (CCK-8, Catalog: G021-1-1). After hypoxia had ended, the anoxic solution containing CoCl₂ was discarded, and the cells were washed three times with phosphate-buffered saline (PBS, Catalog: 003,002). Then, the high-glucose DMEM containing 10% FBS was used for reoxygenation for 1, 2, 3, 4, 5, and 6 hr, respectively. According to the results of the CCK-8 kits, the optimal reoxygenation time was determined. Based on the above results, the H/R model was established.

2.4 | Experimental treatment

H9c2 cardiomyocytes were randomly divided into the four groups: the control group (CONT, normal cultured cells); the H/R group (H/R, after 24-hr incubation with 600 μ mol/L of CoCl₂ solution, the anoxic solution was discarded, and the culture was continued in normal medium for 3 hr); the low-dose 10-Gin pretreatment group (L-10-Gin, cells were pretreated with 10-Gin at 10 μ mol/L for 24 hr, other steps are consistent with the H/R group); and the high-dose 10-Gin pretreatment group (H-10-Gin, cells were pretreated with 10-Gin at 30 μ mol/L for 24 hr, other steps are consistent with the H/R group).

2.5 | Detection of H9c2 cardiomyocyte activity by CCK-8 assay

The CCK-8 assay was used to detect the effects of 10-Gin (10, 20, 30, 40, 50, and 60 μ mol/L) on the viability of H9c2 cardiomyocytes cultured in 96-well plates. Briefly, according to the manufacturer's instructions, when the cells had grown to 80% confluence, different concentrations of 10-Gin were added into the plate treated for 24 hr in 5% CO₂ and 95% air at 37 °C. Then, 100 μ L/well culture medium and 10 μ L/well CCK-8 solution were added to each well, and the cells were incubated for a further 2 hr at 37 °C. Absorbance was measured at 450 nm with an enzyme labeling instrument (Thermo Scientific Varioskan LUX, Thermo Fisher Scientific, Inc.). The hypoxia concentration of CoCl₂ was determined as 600 μ mol/L, and the concentrations

of the L-10-Gin group and H-10-Gin group were determined to be 10 μ mol/L and 30 μ mol/L, respectively. Then, according to the experimental treatment, the viability of H9c2 cardiomyocytes in each group was detected after the experimental procedure.

2.6 | Assessment of lactated dehydrogenase (LDH) and creatine kinase (CK)

After the experimental procedure, the cell culture supernatant of the four groups was collected and centrifuged at 645 \times g for 10 min. After centrifugation, 100 μ L/well of supernatant was added in 96-well plates, and the activities of LDH (Catalog: A020-2-2) and CK (Catalog: A032-1-1) in each group were detected according to the kit instructions.

2.7 | Detection of oxidative stress levels

After the experimental treatments, the cells were digested with an appropriate amount of trypsin and centrifuged at 645 \times g for 10 min. The supernatant was discarded, and 500 μ L PBS solution was added to the cell precipitation to resuspend and mix. Then, the cells were ruptured under the condition of ultrasound for 2 s and repeated ten times to obtain a crushed cell homogenate. The levels of superoxide dismutase (SOD, Catalog: A001-3-2), catalase (CAT, Catalog: A007-1-1), glutathione (GSH, Catalog: A006-2-1), and malondialdehyde (MDA, Catalog: A003-1-1) in the cell homogenate were determined according to the instructions of the kit.

2.8 | Measurement of reactive oxygen species (ROS) generation

2,7-Dichlorodihydrofluorescein diacetate (DCFH-DA, Cayman Chemical, Michigan, USA, Catalog: 85,155) is a common dichlorofluorescein used as an indicator of peroxynitrite formation. Briefly, after the experimental procedure, the supernatant of cultured cells in a 24-well plate was discarded, and 500 μ L/well of DCFH-DA dye was added into each group. The cells were incubated in the dark at 37 °C for 20 min. Next, the dye was removed, and the cells were twice rinsed with PBS, and a fluorescence microscope was used for fluorescence image collection. Image-Pro Plus 6.0 software (Media Cybernetics, Inc.) was used for quantification.

2.9 | Analysis of [Ca²⁺]_i concentration by Fluo-3 a.m. staining

The cells were inoculated in 24-well plates, and the Fluo-3 a.m. (Catalog: F1242) concentration was diluted to 10 μ mol/L according to the instructions of the Ca²⁺ GPCR assay calcium ion indicating probe kit. Then, 500 μ L/well of dye was added to each well and incubated at 37 °C in the dark for 20 min. Next, the dye was removed,

and the cells were rinsed with PBS twice, and a fluorescence microscope was used for fluorescence image collection. Image-Pro Plus 6.0 software was used for quantification.

2.10 | Assay of MMP by Rhodamine 123 (Rh123) staining

Cell mitochondria can rely on their membrane electronegative to assimilate the cationic fluorescent dyeing Rh123 (Shanghai Yuanye

Biotechnology, Shanghai, China, Catalog: S19123). Damage to a cell's MMP can result in reduced uptake capacity of Rh123. Therefore, the mitochondrial function can be indirectly inferred from the intake of Rh123. Briefly, after the experimental procedure, the supernatant of cultured cells in a 24-well plate was discarded, and 500 μL /well of Rh123 (10 $\mu\text{g}/\text{mL}$) dyeing was added into each group. The cells were incubated in the dark at 37 $^{\circ}\text{C}$ for 15 min. Next, the dye was removed, and the cells were rinsed twice with PBS, and a fluorescence microscope was used for fluorescence image collection. Image-Pro Plus 6.0 software was used for quantification.

TABLE 1 Detection of target gene primers by real-time PCR

Primer	Sequences (5'→3')
Wnt5a	Forward: GGACTTACCTCGGGACTGG
	Reverse: CGACCTGCTTCATTGTTGTG
Frizzled-2	Forward: GCAGGCACTAAGAA AGAA
	Reverse: ACCAGGTGAGGGACAGAA
β -actin	Forward: CGTTGACATCCGTAAGAC
	Reverse: TAGGAGCCAGGGCAGTA

2.11 | Detection of intracellular inflammatory cytokines

After the experimental treatments, the cells were digested with an appropriate amount of trypsin and centrifuged at 645 $\times g$ for 10 min. The supernatant was discarded, and 500 μL PBS solution was added to the cell precipitation to resuspend and mix. Then, the cells were ruptured under the condition of ultrasound for 2 s and repeated ten times to obtain the crushed cell homogenate. The crushed cell

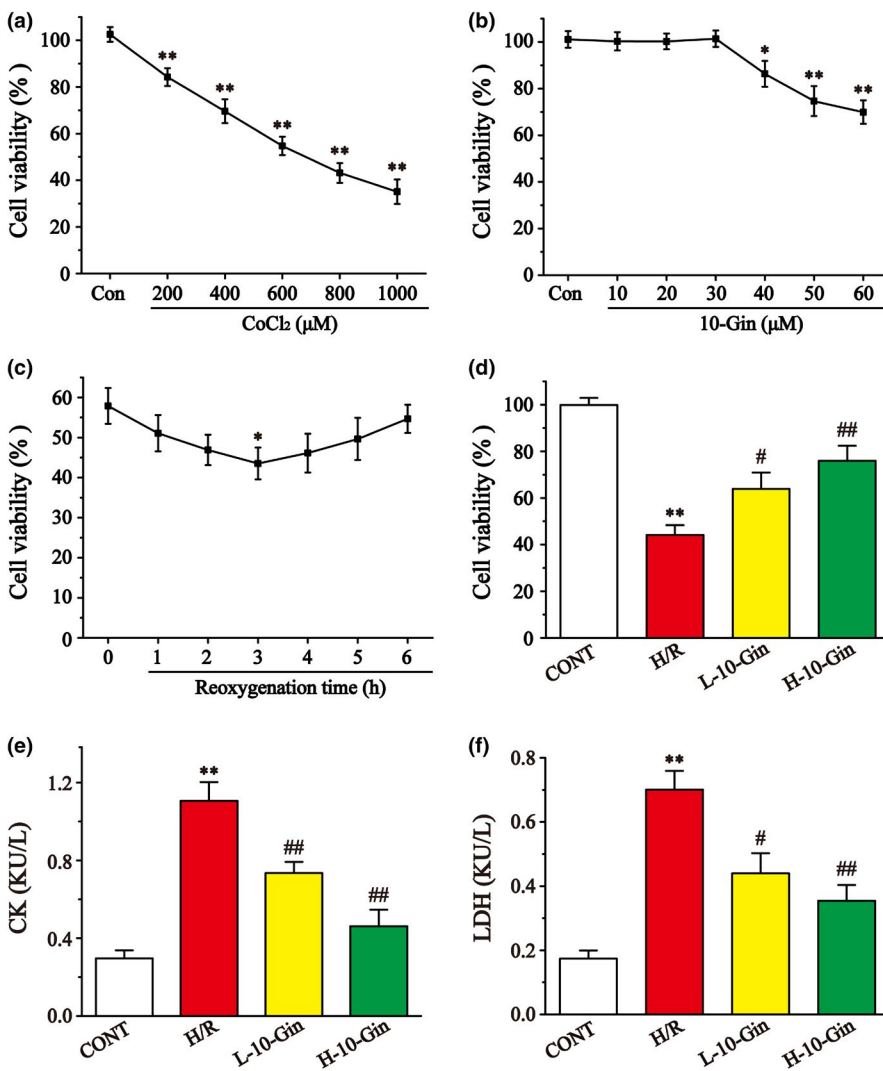


FIGURE 2 Effects of CoCl₂ and 10-Gin on the vitality of H9c2 cells by CCK-8 assay, and effects of 10-Gin on CK (e) and LDH (f). H9c2 cells were incubated with different concentrations of CoCl₂ (a) and 10-Gin (b) for 24 hr, followed by reoxygenation (c). The vitality of H9c2 cells in each group is shown by the CCK-8 assay (d). Data are represented as mean \pm SEM. * $p < .05$, ** $p < .01$ versus. CONT; # $p < .05$, ## $p < .01$ versus. H/R group, $n = 6$

homogenate was collected as samples to be tested, and the levels of interleukin-6 (IL-6, Catalog: H007), interleukin-1 β (IL-1 β , Catalog: H002), and tumor necrosis factor- α (TNF- α , Catalog: H052) were determined according to the kit instructions.

2.12 | Assessment of apoptosis by flow cytometry and Hoechst-33258 staining

An Annexin V-FITC/PI apoptosis detection kit (Catalog: G003-1-3) was used to detect cell apoptosis. After the experimental procedure, the cells of the different treatment groups were collected and washed three times with PBS. Then, the cells were resuspended with a prepared binding buffer (100 μ L) and adjusted to a density of 1×10^6 /ml. 100 μ L of cell suspension was inoculated into a 5-mL flow tube and stained with 5 μ L Annexin V-FITC and 5 μ L PI that incubate away from light at room temperature for 15 min. Finally, the apoptosis rate was analyzed by flow cytometry (Beckman FC500, Beckman Coulter, Inc.).

Hoechst-33258 (Beijing Solarbio Science & Technology, Beijing, China, Catalog: IH0060) is a specific DNA dye that can detect cell apoptosis through fluorescence intensity. After the experimental procedure, the cell culture medium of 24-well plates in each group was discarded, and H9c2 cardiomyocytes were washed three times with PBS. Then, 500 μ L/well of Hoechst-33258 staining solution (10 μ g/mL) was added to each group of cells and incubated at 37 $^{\circ}$ C for 20 min. Next, the dye was removed, and the cells were rinsed twice with PBS, and a fluorescence microscope was used for fluorescence image collection. Image-Pro Plus 6.0 software was used for quantification.

2.13 | Measurement of Caspase-3 activity

After the experimental procedure, the supernatant of each treatment group was discarded, and the lysate provided by the kit was added, and the cells of each group were incubated on ice for 15 min. Then, the cells were centrifuged at $12,000 \times g$ for 15 min. The supernatant was collected and stored at -80° C. In strict accordance with the kit's instructions, the protein samples were mixed with the substrate in a 37 $^{\circ}$ C water bath for 1 hr, and the absorbance of the fluorescent substrate was determined at 405-nm wavelength. The activity of caspase-3 (Catalog: G015-1-3) was calculated according to the kit instructions.

2.14 | Real-time polymerase chain reaction (RT-PCR)

SYBR Green I RT-PCR was used to detect the changes in the mRNA transcription level of the target gene in the samples. Total RNA was extracted from cell samples using TRIzol (Ambion, Thermo Fisher Scientific, Inc., Catalog: 15,596,018), and 1 μ L RNA was taken to measure the quality and concentration of RNA and to detect RNA integrity. Reverse transcription was carried out in a volume of 20 μ L containing 1 μ g total RNA. The expression of Wnt5a, Frizzled-2, and β -actin in H9c2 cells was quantitatively detected by quantitative fluorescence PCR, and the relative quantitative analysis of the data was carried out by the $2^{-\Delta\Delta CT}$ method. The PCR conditions were as follows: 40 cycles at 95 $^{\circ}$ C for 1 min, 95 $^{\circ}$ C for 15 s, and 55 $^{\circ}$ C for 1 min. β -Actin was used as an internal reference. The primer sequence is shown in Table 1.

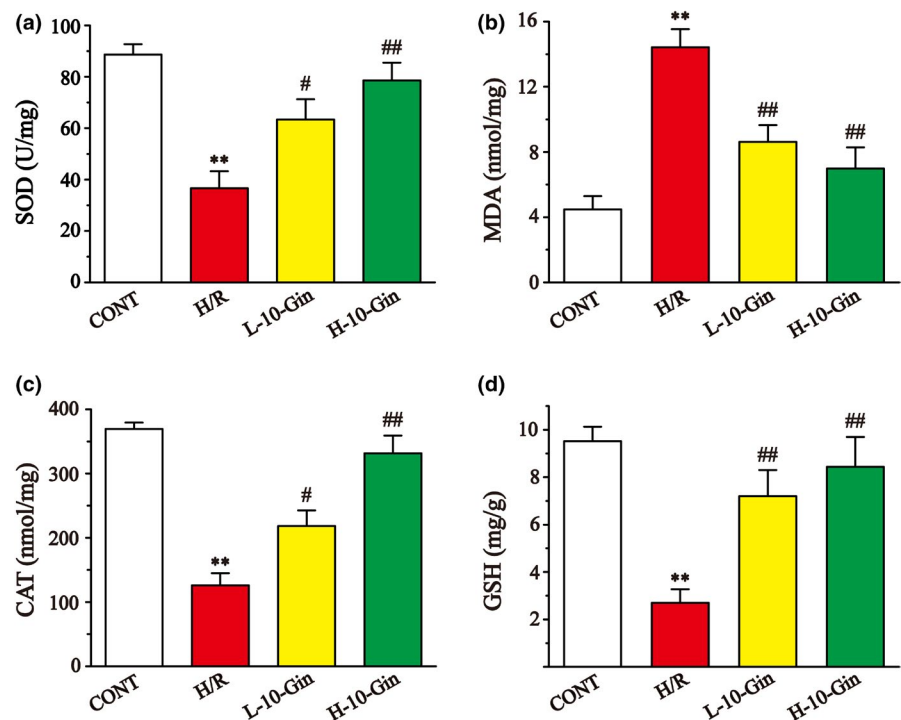


FIGURE 3 Effects of 10-Gin on the levels of SOD (a), MDA (b), CAT (c), and GSH (d). Data are represented as mean \pm SEM. ** $p < .01$ versus. CONT; # $p < .05$, ## $p < .01$ versus. H/R group, $n = 6$

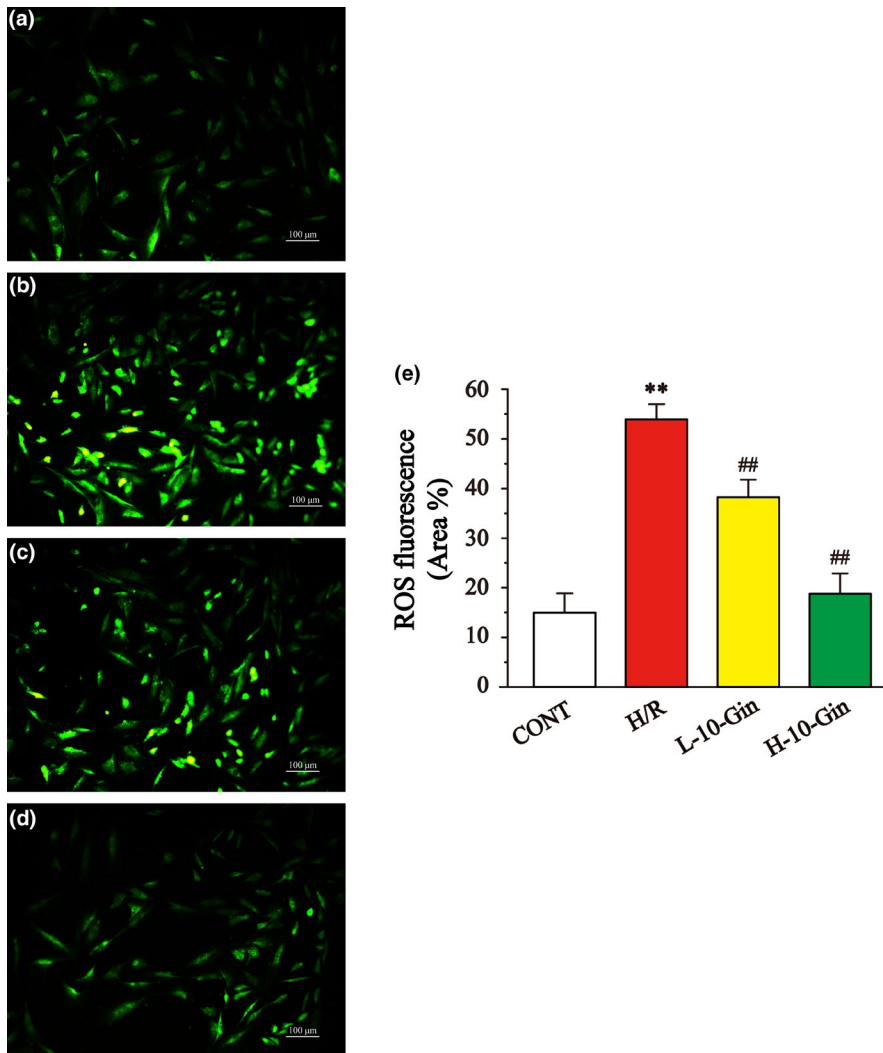


FIGURE 4 Effects of 10-Gin on levels of ROS. ROS fluorescence images of different groups (a) CONT group; (b) H/R group; (c) L-10-Gin treatment group; and (d) H-10-Gin treatment group) and the ratio graph E about ROS fluorescence intensity are presented. Scale bar = 100 μ m (200 \times). Data are represented as mean \pm SEM. ** $p < .01$ versus. CONT; ## $p < .01$ versus. H/R group, $n = 6$

2.15 | Western blot analysis

The protein expression levels of Wnt5a and Frizzled-2 were measured by Western blotting. After the experimental procedure, cells in each group were rinsed three times with precooled PBS, and RIPA lysate (Beijing Solarbio Science & Technology, Beijing, China, Catalog: R0020) was added and incubated overnight at 4 $^{\circ}$ C, then centrifuged at 12,000 \times g for 10 min. The supernatant was taken, and the Wnt5a, Frizzled-2, and β -actin protein contents in the sample were detected by Coomassie Brilliant Blue Reagent Kit (Shanghai Yuanye Biotechnology, Shanghai, China, Catalog: R21271). Protein buffer was added for protein denaturation and electrophoresis. The separated protein bands were fixed on polyvinylidene difluoride membrane (Millipore Sigma, Inc., Catalog: IPVH00010), and the transfer times were as follows: Frizzled-2, 45 min; Wnt5a, 37 min; and β -actin, 37 min. The membrane was then sealed with skimmed milk, then reacted overnight at 4 $^{\circ}$ C with rabbit anti-Wnt5a (Affinity Biosciences, Jiangsu, China; diluted at 1:1,000, Catalog: DF6856), rabbit anti-Frizzled-2 (Affinity Biosciences, Jiangsu, China; diluted at 1:500, Catalog: AF5282), and rabbit anti- β -actin (Affinity Biosciences, Jiangsu, China; diluted at 1:1,000, Catalog: AF7018), respectively. After washing three times with 1 \times PBST, the horseradish peroxidase-labeled secondary diluted antibodies

(1:3,000) were incubated at room temperature for 90 min to develop color. The Tanon GIS software measured the gray value of the strip (Tanon, Inc., Shanghai, China) after the film was scanned.

2.16 | Statistical analyses

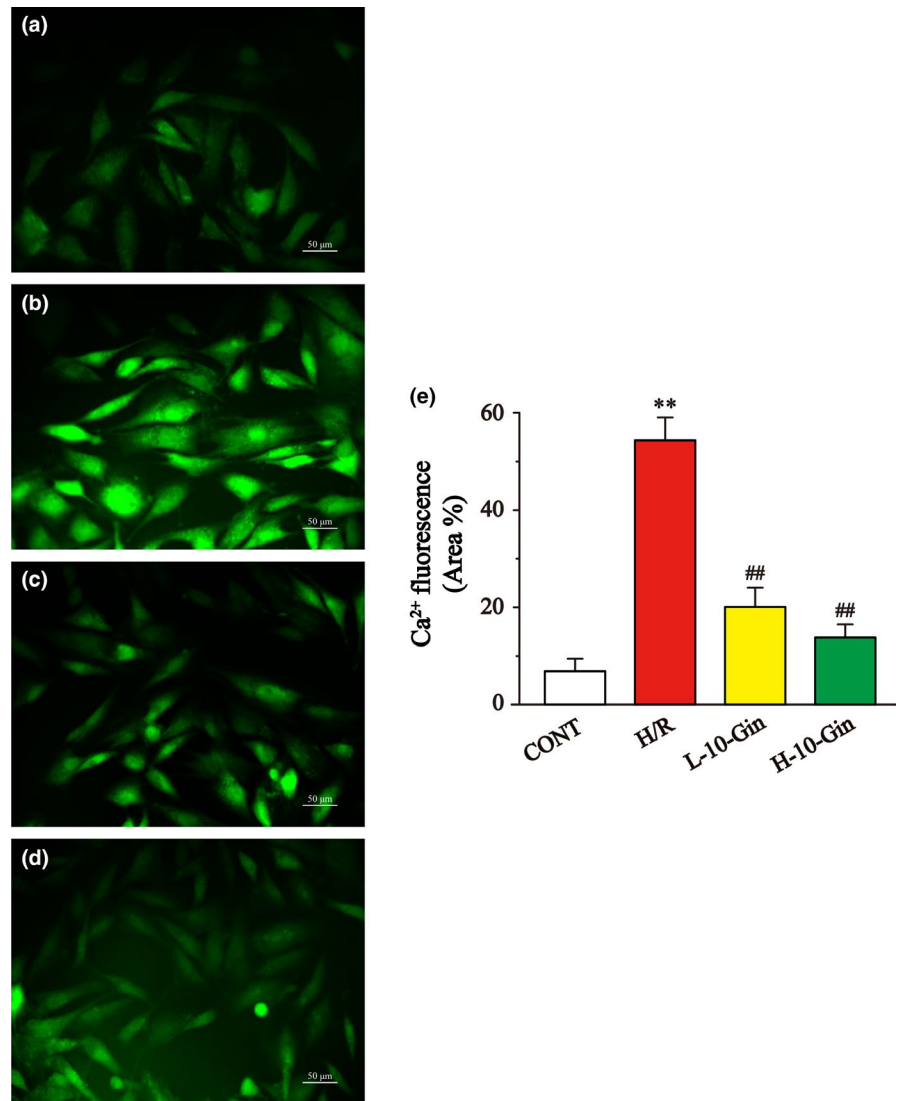
The measurement values are shown as the mean \pm standard error of the mean (SEM), and the differences in data among groups were analyzed via one-way analysis of variance (ANOVA) followed by Tukey's test using the Origin 7.5 software (OriginLab, Inc.). P -values < 0.05 were considered statistically significant.

3 | RESULTS

3.1 | Effects of 10-Gin on cell viability

The results of H9c2 cardiomyocyte cytotoxicity show that 600 μ mol/L CoCl_2 and 40 μ mol/L 10-Gin could significantly inhibit the viability of the H9c2 cells (Figure 2a and 2b) ($p < .05$ or $p < .01$). Therefore, 600 μ mol/L

FIGURE 5 Effects of 10-Gin on $[Ca^{2+}]_i$ concentration of H/R cardiomyocytes by flow-3 staining. $[Ca^{2+}]_i$ fluorescence images of different groups (a) CONT group; (b) H/R group; (c) L-10-Gin treatment group; and (d) H-10-Gin treatment group) and the ratio graph (e) about $[Ca^{2+}]_i$ fluorescence intensity are presented. Scale bar = 50 μ m (400 \times). Data are represented as mean \pm SEM. ** $p < .01$ versus. CONT; ## $p < .01$ versus. H/R group, $n = 6$



CoCl₂ (Figure 2a) was determined as the hypoxia concentration, and 10 μ mol/L and 30 μ mol/L-10-Gin (Figure 2b) were determined as the low- and high-dose group concentrations, respectively. Figure 2c shows that the cell viabilities were in a U-shape, indicating that the maximum damage occurred at the third hour after reoxygenation. Figure 2d shows that the cell viability in the H/R group was obviously reduced compared with the CONT group ($p < .01$). But 10-Gin treatment could reverse the situation compared with the H/R group, showing that 10-Gin could protect against the cardiomyocyte damage induced by H/R ($p < .05$ or $p < .01$).

3.2 | Effects of 10-Gin on CK and LDH

Figure 2e and 2f shows that the levels of CK and LDH were detected to assess H9c2 cardiomyocyte injury induced by H/R. Compared with the CONT group, the activities of CK and LDH in the H/R group were obviously increased ($p < .01$). But 10-Gin treatment significantly decreased the activities of CK and LDH compared with the H/R group, suggesting that pretreatment with 10-Gin can reduce the cardiomyocyte damage induced by H/R ($p < .05$ or $p < .01$).

3.3 | Effects of 10-Gin on oxidative stress

The levels of SOD, CAT, GSH, and MDA are shown in Figure 3. The levels of SOD, CAT, and GSH in the H/R group were lower than the CONT group ($p < .01$), while the content of MDA was higher ($p < .01$). However, the levels of SOD, CAT and GSH in the 10-Gin treatment group were obviously increased compared with the H/R group ($p < .05$ or $p < .01$), while the levels of MDA were observably decreased ($p < .01$), showing that 10-Gin could protect against oxidative stress injury induced by H/R.

3.4 | Effects of 10-Gin on ROS generation

Figure 4 shows the protective effect of 10-Gin on H/R-induced H9c2 cardiomyocyte injury through measuring ROS levels. Compared with the CONT group, ROS levels in the H/R group were significantly increased ($p < .01$). However, the ROS levels in the 10-Gin treatment group were significantly lower than the H/R group ($p < .01$). These results suggest that 10-Gin can play a protective role by reducing the generation of ROS.

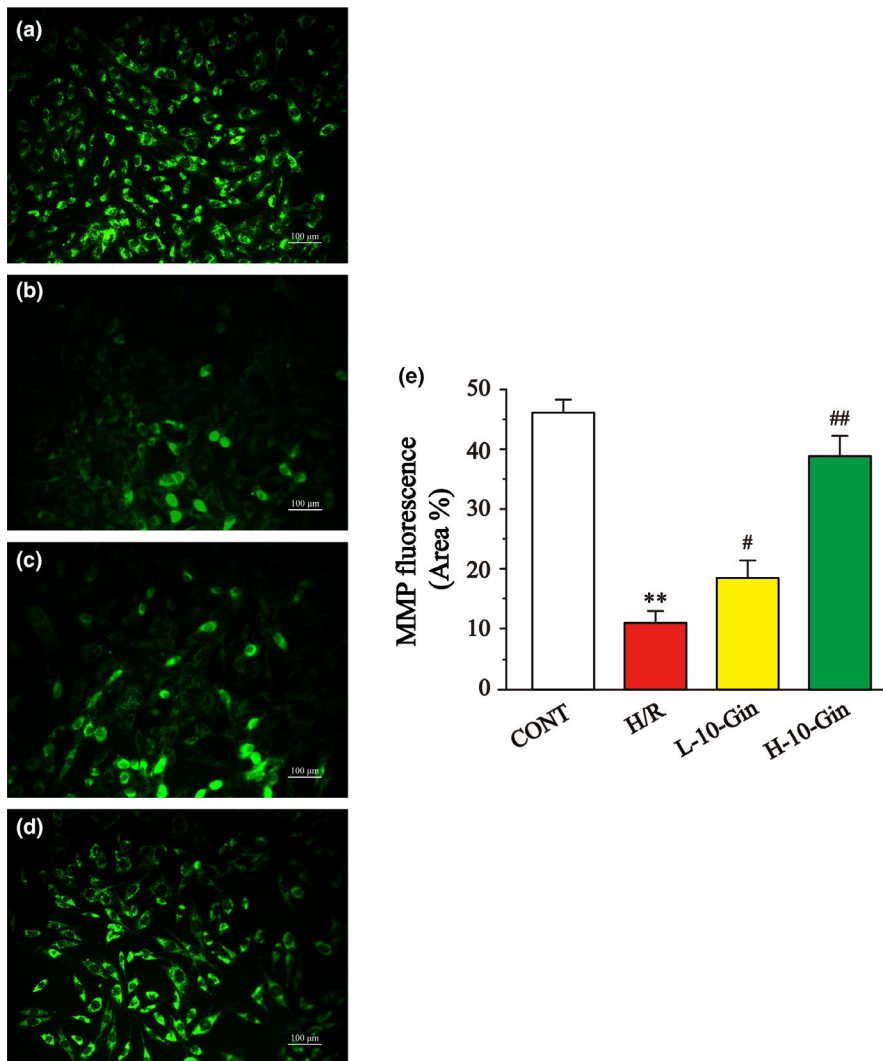


FIGURE 6 Effects of 10-Gin on the MMP. Fluorescence images of different groups (a) CONT group; (b) H/R group; (c) L-10-Gin treatment group; and (d) H-10-Gin treatment group) and the ratio graph (e) about fluorescence intensity are presented. Scale bar =100 μm (200 \times). Data are represented as mean \pm SEM. ** $p < .01$ versus. CONT; # $p < .05$, ## $p < .01$ versus. H/R group, $n = 6$

3.5 | Effects of 10-Gin on $[\text{Ca}^{2+}]_i$ concentration

The results of Figure 5 show that the $[\text{Ca}^{2+}]_i$ concentration in the H/R group was significantly higher than that in the CONT group ($p < .01$). However, the 10-Gin treatment significantly decreased the concentration of $[\text{Ca}^{2+}]_i$ ($p < .01$). These results suggest that 10-Gin has a protective effect on cell injury induced by H/R, and it can be achieved by inhibiting the $[\text{Ca}^{2+}]_i$ concentration.

3.6 | Effects of 10-Gin on MMP

Mitochondria are sensitive to noxious irritation, and their functional status can be reflected by detecting its uptake of fluorescent dye Rh123. As shown in Figure 6, compared with the CONT group, the uptake ability of Rh123 in H9c2 cardiomyocytes of the H/R group was significantly reduced ($p < .01$), suggesting that intracellular mitochondrial was damaged. In contrast, the uptake ability of Rh123 in H9c2 cardiomyocytes of the 10-Gin treatment group was obviously increased relative to the H/R group ($p < .05$

or $p < .01$). These results indicate that 10-Gin could reduce the mitochondrial damage caused by H/R and improve mitochondrial function.

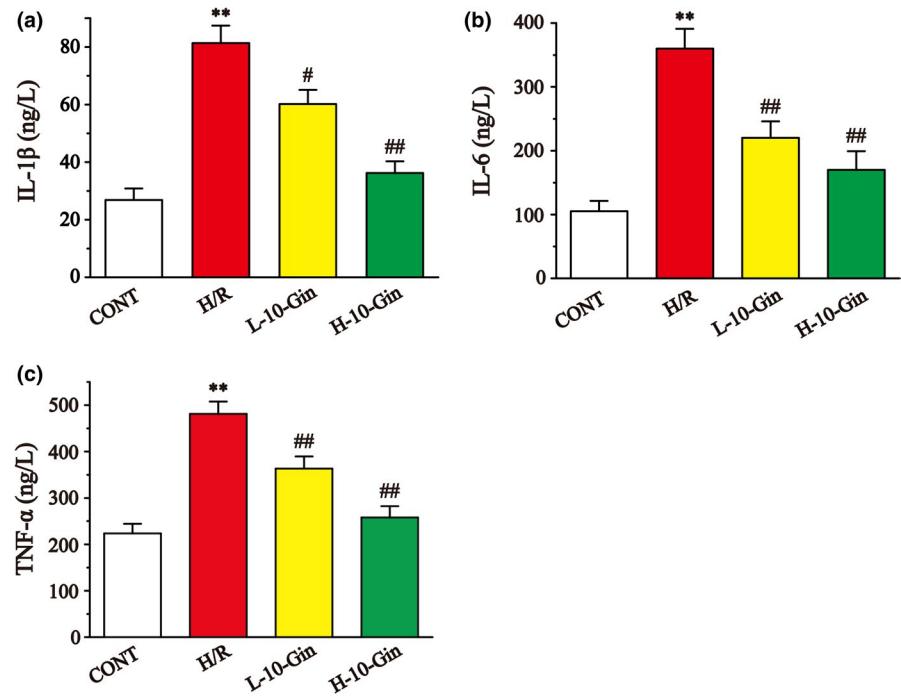
3.7 | Effects of 10-Gin on inflammatory cytokines

Figure 7 shows the levels of IL-1 β , IL-6, and TNF- α . Compared with the CONT group, the levels of IL-1 β , IL-6, and TNF- α in the H/R group were markedly upregulated ($p < .01$). However, 10-Gin treatment significantly reduced the levels of IL-1 β , IL-6, and TNF- α compared with the H/R group ($p < .05$ or $p < .01$). These results indicate that 10-Gin could reduce the inflammatory injury caused by H/R.

3.8 | Effects of 10-Gin on apoptosis

Figure 8 shows the effects of 10-Gin on apoptosis by detecting flow cytometry. The flow cytometry result shows that the apoptosis rate of the H/R group was significantly upregulated compared with

FIGURE 7 Effects of 10-Gin on the levels of IL-1 β (a), IL-6 (b), and TNF- α (c). Data are represented as mean \pm SEM. ** $p < .01$ versus. CONT; # $p < .05$, ## $p < .01$ versus. H/R group, $n = 6$



the CONT group ($p < .01$), while the apoptosis rate of the 10-Gin treatment group was remarkably lower than that of the H/R group ($p < .01$). Meanwhile, the antiapoptotic effect of 10-Gin was further demonstrated by measuring the Hoechst-33258 staining (Figure 9) and using a caspase-3 kit (Figure 9f). The fluorescence intensity and caspase-3 activity of the H/R group were significantly upregulated relative to the CONT group ($p < .01$). However, compared with the H/R group, the 10-Gin treatment significantly decreased the fluorescence intensity and caspase-3 activity ($p < .01$). Therefore, 10-Gin can protect against cardiomyocyte apoptosis induced by H/R.

3.9 | Effects of 10-Gin on the gene and protein expressions of Wnt5a and Frizzled-2

RT-PCR and Western blotting were used to detect the expression of the Wnt5a and Frizzled-2 genes and proteins in H9c2 cardiomyocytes (Figure 10). The gene and protein expressions of Wnt5a and Frizzled-2 in the H/R group were significantly increased compared with the CONT group ($p < .01$). However, 10-Gin treatment was markedly decreased compared with the H/R group ($p < .05$ or $p < .01$). These results suggest that 10-Gin has a protective effect on H9c2 cardiomyocytes by inhibiting the expression of Wnt5a and Frizzled-2 genes and proteins.

4 | DISCUSSION

As the main active ingredient in ginger, gingerol has been reported to have a myocardial protective effect (Namekata et al., 2008; Maier et al., 2000). However, there are no studies reporting that 10-Gin can protect against MIRI. This study shows that 10-Gin increased

the viability of H9c2 cells in the H/R model (Figure 2d). Furthermore, we explored the protection of 10-Gin treatment on H/R-induced injury through oxidative stress, inflammation, and apoptosis, and its related signal pathways were also explored.

CoCl₂ is commonly used for chemical hypoxia simulation in in vitro experiments (Jung et al., 2007). Co²⁺ in CoCl₂ has a low affinity for oxygen, which can bind to oxygen by replacing Fe²⁺ in the hemo-globin protein porphyrin ring, causing cell hypoxia (Xiao et al., 2012). H9c2 cardiomyocytes are a kind of cardiac cell line isolated from the embryonic heart of rats with morphological characteristics similar to those of embryonic rat cardiomyocytes (Hescheler et al., 1991). H9c2 cardiomyocytes also have similar electrophysiological characteristics to rat cardiomyocytes (Eguchi et al., 2008). Therefore, the H/R model was established by treating H9c2 cardiomyocytes with 600 μ mol/L CoCl₂ for 24 hr and reoxygenating for 3 hr (Figure 2a-c). CK and LDH are stable cytosolic enzymes that exist in cardiomyocytes (Muders et al., 2001). When the myocardial cell membrane is damaged, CK and LDH are rapidly released from the cells into the cell culture medium (Muders et al., 2001). Therefore, CK and LDH kits can be used to detect the cell damage caused by H/R. In the present study, 10-Gin treatment significantly decreased the CK and LDH activities, proving that 10-Gin offers protection against H/R-induced cardiomyocyte injury (Figure 2e and 2f).

The function of the OFR scavenging system is reduced during reperfusion, while the activity of the OFR generating system is gradually enhanced, leading to a large increase in OFR, which causes serious oxidative stress damage to cardiomyocytes (Hess & Manson, 1984). SOD and CAT, as the main enzymes in the antioxidant system, can inhibit the further development of oxidative stress (Wang et al., 2017). GSH is an abundant and ubiquitous low-molecular-weight thiol that has been proposed to have roles in many cellular processes, including protection against the deleterious

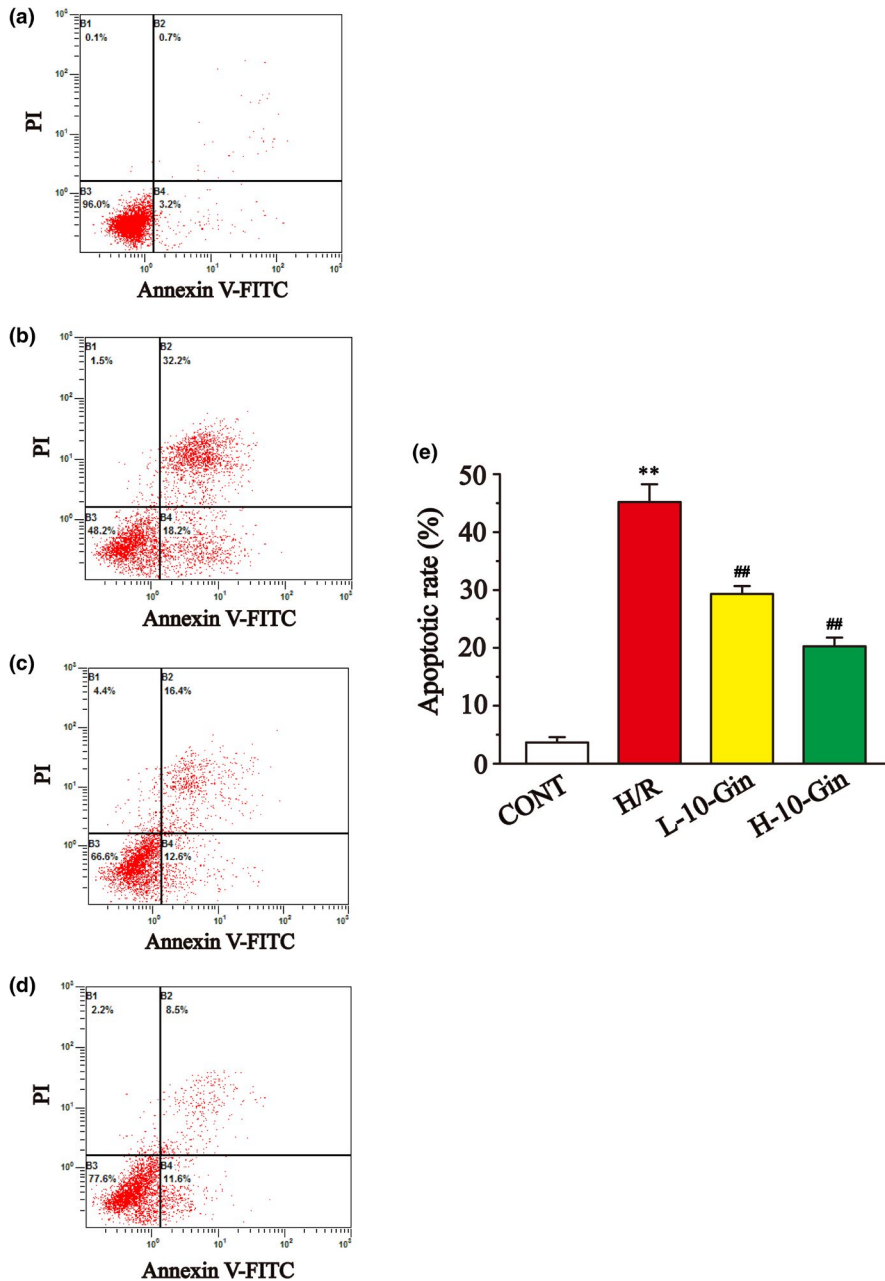


FIGURE 8 Effects of 10-Gin on cell apoptosis of H/R cardiomyocytes by flow cytometry. Apoptotic images of different groups (a) CONT group; (b) H/R group; (c) L-10-Gin treatment group; and (d) H-10-Gin treatment group and the ratio graph E about apoptotic rate are presented. Data are represented as mean \pm SEM. ** $p < .01$ versus. CONT; ## $p < .01$ versus. H/R group, $n = 3$

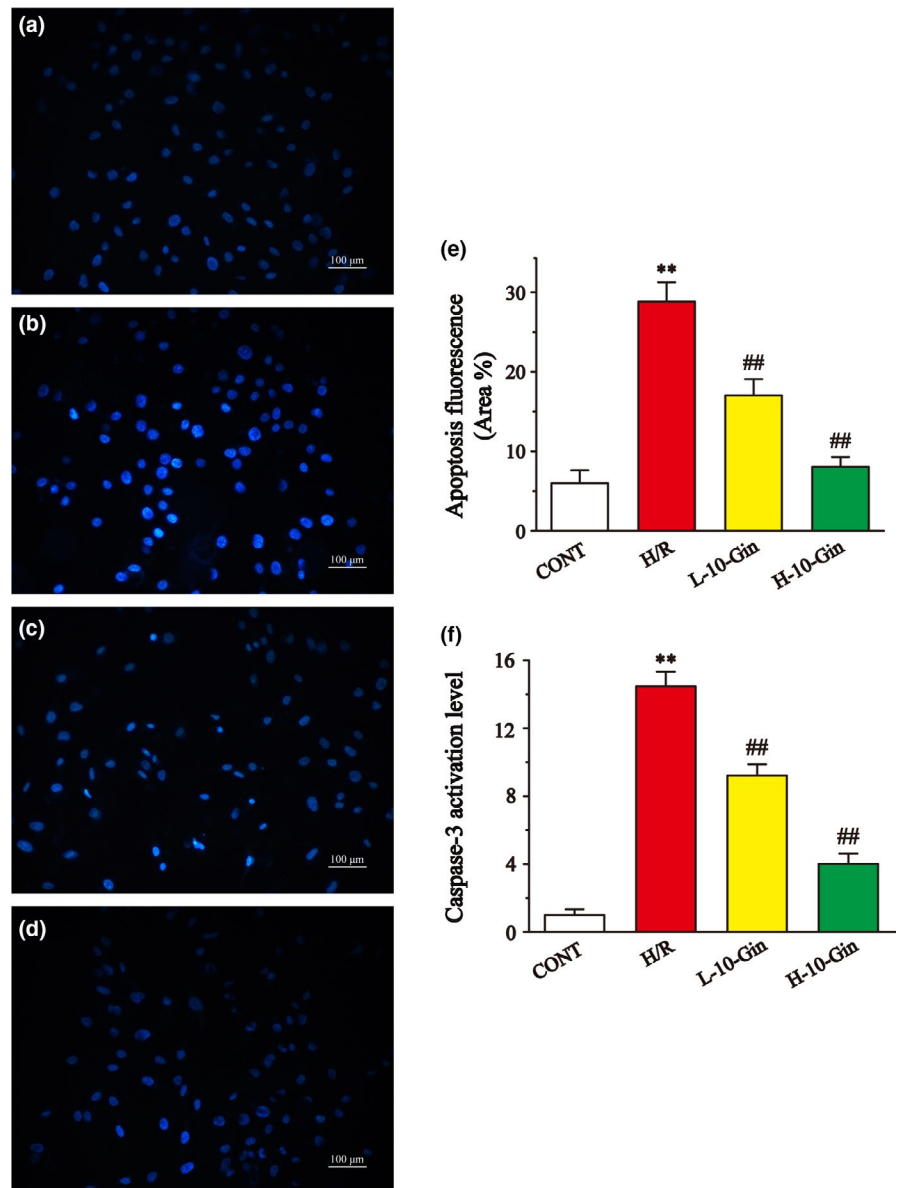
effects of ROS (Grant et al., 1998). The level of MDA could reflect the degree of lipid peroxidation, thereby indirectly reflecting the degree of cell injury (Del Rio et al., 2005). SOD could convert superoxide anion produced by lipid peroxidation into H_2O_2 , and CAT and GSH transform H_2O_2 into oxygen and water, so the activities of these three enzymes are tested to explore the damage degree of the antioxidant system (Aruoma & Halliwell, 1987; Hoekstra et al., 2003). In this study, the SOD, CAT, GSH, and MDA data prove that the 10-Gin treatment could significantly reduce the oxidative stress level, showing that 10-Gin protects against H9c2 cardiomyocyte injury induced by H/R through antioxidant stress effects (Figure 3).

The generation of oxidative stress injury is closely related to myocardial ischemia/hypoxia (Giordano, 2005). ROS are a series of cell molecules produced in the process of oxygen metabolism and important mediators in oxidative stress injury (Del Rio et al., 2005).

As the main site of ROS production, mitochondria play an important role in MIRI (Madungwe et al., 2016). During MIRI, mitochondrial function might be affected by $[Ca^{2+}]_i$ overload (Hurst et al., 2017). Also, the opening of mPTP is a key determinant of mitochondrial dysfunction (Weiss et al., 2003). When mPTP is turned on, free solutes and proteins can be distributed in the mitochondrial inner membrane, causing MMP to collapse (Kroemer, 1999). The opening of mPTP causes mitochondrial dysfunction, leading to ATP depletion and ultimately to cardiomyocyte apoptosis (Li et al., 2017; Whelan et al., 2010). Therefore, H/R-induced mitochondrial dysfunction can be improved by inhibiting $[Ca^{2+}]_i$ overload, preventing the excessive production of ROS, blocking the opening of mPTP, increasing MMP, and reducing ATP consumption.

This study shows that the ROS of H9c2 cardiomyocytes stimulated by H/R was significantly increased compared with the CONT

FIGURE 9 Effects of 10-Gin on cell apoptosis of H/R cardiomyocytes by Hoechst 33,258 staining and caspase-3 kit. Apoptotic fluorescence images of different groups (a) CONT group; (b) H/R group; (c) L-10-Gin treatment group; and (d) H-10-Gin treatment group, the ratio graph (e) about apoptotic fluorescence intensity, and the graph F about caspase-3 activity are presented. Scale bar =100 μ m (200 \times). Data are represented as mean \pm SEM. ** $p < .01$ versus. CONT; ## $p < .01$ versus. H/R group, $n = 6$



group (Figure 4). Meanwhile, the uptake ability of Rh123 in H9c2 cardiomyocytes of the H/R group was significantly reduced, suggesting that intracellular MMP was reduced (Figure 6). However, 10-Gin treatment can significantly reduce the level of ROS and increase MMP. Moreover, we used Fluo-3 a.m. fluorescent dye to measure the Ca^{2+} concentration in H9c2 cardiomyocytes and showed the $[Ca^{2+}]_i$ concentration through the fluorescence intensity. Our results show that 10-Gin treatment can significantly reduce the $[Ca^{2+}]_i$ concentration, indicating that 10-Gin has a protective effect on H/R-induced $[Ca^{2+}]_i$ overload injury (Figure 5).

Inflammation can cause substantial cell damage and organ dysfunction, which is another important cause of MIRI (Li et al., 2002). In MIRI-induced inflammation, TNF- α can mediate the release of other inflammatory factors, such as IL-6, leading to a cascade of inflammation and aggravating cell damage (Hu et al., 2016). Among these, the high concentration of IL-6 will activate neutrophils, lymphocytes,

and macrophages and induce oxidative damage to the myocardium (Jian et al., 2016). IL-1 β can induce cell apoptosis and promote cardiomyocyte remodeling (Zhu et al., 2019). In this experiment, the levels of TNF- α , IL-1 β , and IL-6 were measured by the ELISA method. Our results show that the 10-Gin pretreatment effectively reduced the production of TNF- α , IL-1 β , and IL-6, suggesting that 10-Gin could reduce the inflammatory response to produce myocardial protection (Figure 7).

The cascade activation of caspase is an important mechanism in cell apoptosis (Moorjani et al., 2009). Caspase-3, as the final common pathway of apoptosis, is an important sign of apoptosis (Arumugam et al., 2006). Also, $[Ca^{2+}]_i$ overload can indirectly induce apoptosis by damaging mitochondria and promoting the generation of free radicals (Scarabelli et al., 2002). In this study, our flow cytometry and apoptotic fluorescence results show that the 10-Gin treatment could significantly reduce the apoptosis of H9c2 cardiomyocytes

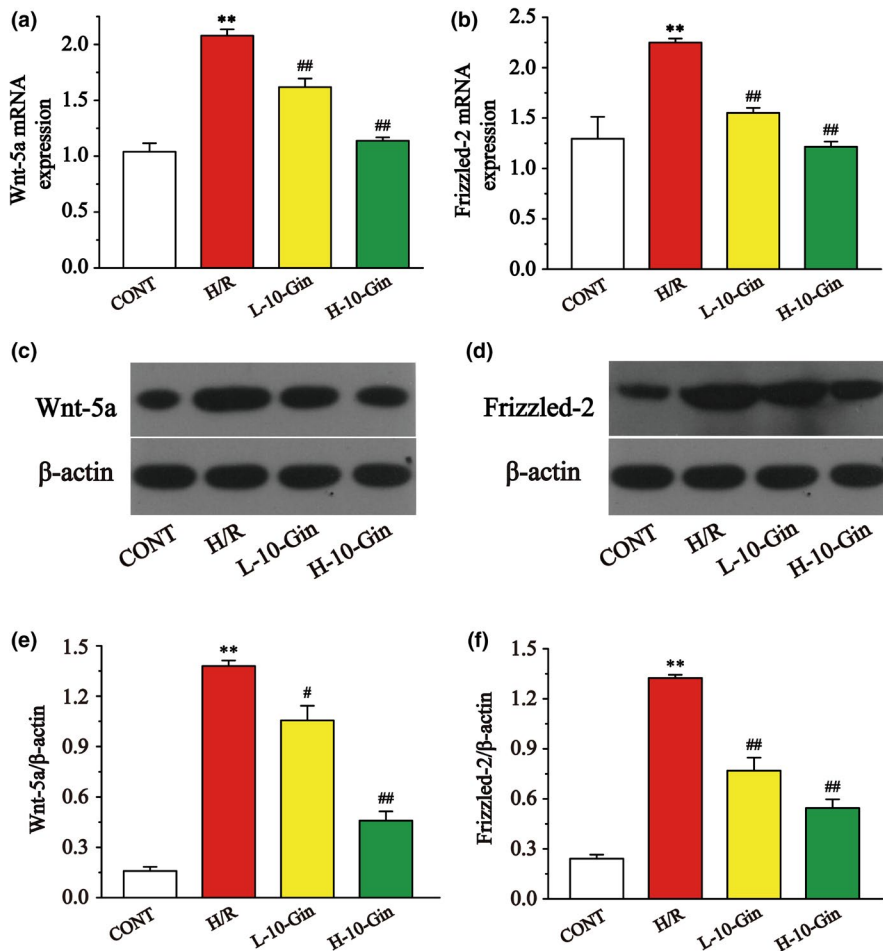


FIGURE 10 Effects of 10-Gin on the Wnt5a (a, c, e) and Frizzled-2 (b, d, f) gene and protein expressions. Data are represented as mean \pm SEM. ** $p < .01$ versus. CONT; # $p < .05$, ## $p < .01$ versus. H/R group, $n = 3$

caused by H/R (Figures 8 and 9). Also, the 10-Gin treatment also clearly reduced the level of caspase-3, further supporting the antiapoptotic effect of 10-Gin (Figure 9f).

Wnt is a glycoprotein family member and an important extracellular signaling factor. As a ligand, Wnt can combine with the corresponding receptor in the Frizzled family, bringing about corresponding effects on cell differentiation and cell proliferation (De, 2011). As the cell surface receptor of Wnt5a, Frizzled-2 combines with Wnt5a to activate the downstream transduction signal and promote the release of $[Ca^{2+}]_i$ (Gasser, 1988). Therefore, the Wnt5a/Frizzled-2 pathway is also known as the Wnt/ Ca^{2+} pathway. The Wnt5a/Frizzled-2 pathway can be activated upon ischemia/anoxia stimulation (Blankesteyn et al., 1997). It is worth noting that a study has reported that when the rat Frizzled-2 gene is ectopically expressed in the zebrafish embryo cell, the coexpression of Wnt5a is increased (Slusarski and Yang-Snyder et al., 1997) and that the increased free Ca^{2+} comes from the Ca^{2+} pool of the mitochondria and endoplasmic reticulum. In this study, the gene and protein expression levels of Wnt5a and Frizzled-2 were examined to demonstrate that 10-Gin inhibits $[Ca^{2+}]_i$ overload through inhibiting the Wnt5a/Frizzled-2 pathway. Our results demonstrate that 10-Gin treatment significantly decreases the gene and protein expression levels of Wnt5a and Frizzled-2 (Figure 10).

In this study, the H/R-induced H9c2 cardiomyocyte injury model was used to mimic MIRI, and the cardiomyocytes were pretreated with different concentrations of 10-Gin. The results showed that 10-Gin attenuated oxidative stress, inflammatory response, apoptosis damage, and decreased $[Ca^{2+}]_i$ concentration. Although the H9c2 cell line is commonly used in in vitro studies of heart-related diseases due to its similar current physiology, biochemistry, and other properties as primary cardiomyocytes (Zhu et al., 2017), it is still different from primary cardiomyocytes, such as cell morphology, cell contractility, and gene expression (Hescheler et al., 1991; Xie et al., 2016; Zhu et al., 2017). In addition, the heart is regulated by many mechanisms including neurotransmitters and body fluids in vivo, the mechanisms are complex and cannot be manifested in in vitro. The investigations of the present study are limited to the cellular level, so in vivo experiments should be conducted to further explore the protective effects of 10-Gin on MIRI.

5 | CONCLUSIONS

In conclusion, 10-Gin can attenuate the injury caused by H/R and reduce oxidative stress, $[Ca^{2+}]_i$ overload, inflammation, and apoptosis, which is related to the inhibition of the Wnt5a/Frizzled-2 pathway.

Our research provides an experimental basis and new treatment strategies for MIRI. However, further research will be needed before these treatments can be used in clinics.

ACKNOWLEDGMENTS

This trial was supported by the Project of Science and Technology Research Project of Hebei Province, China (No. BJ2020002).

CONFLICTS OF INTEREST

The authors declare that they do not have any conflict of interest.

ETHICAL APPROVAL

This study does not involve any human or animal testing.

DATA AVAILABILITY STATEMENT

The datasets used and/or analyzed during the current study are available from the corresponding author on reasonable request.

ORCID

Li Chu  <https://orcid.org/0000-0002-6301-2709>

REFERENCES

- Aissaoui, N., Puymirat, E., Delmas, C., Ortuno, S., Durand, E., Bataille, V., Drouet, E., Bonello, L., Bonnefoy-Cudraz, E., Lesmeles, G., Guerot, E., Schiele, F., Simon, T., & Danchin, N. (2020). Trends in cardiogenic shock complicating acute myocardial infarction. *European Journal of Heart Failure*, 22(4), 664–672. <https://doi.org/10.1002/ejhf.1750>
- Aldakkak, M., Camara, A. K., Heisner, J. S., Yang, M., & Stowe, D. F. (2011). Ranolazine reduces Ca²⁺ overload and oxidative stress and improves mitochondrial integrity to protect against ischemia reperfusion injury in isolated hearts. *Pharmacological Research*, 64(4), 381–392. <https://doi.org/10.1016/j.phrs.2011.06.018>
- Ali, B. H., Blunden, G., Tanira, M. O., & Nemmar, A. (2008). Some phytochemical, pharmacological and toxicological properties of ginger (*Zingiber officinale* Roscoe): A review of recent research. *Food Chemical Toxicology*, 46(2), 409–420. <https://doi.org/10.1016/j.fct.2007.09.085>
- Arumugam, T. V., Chan, S. L., Jo, D. G., Yilmaz, G., Tang, S. C., Cheng, A., Gleichmann, M., Okun, E., Dixit, V. D., Chigurupati, S., Mughal, M. R., Ouyang, X., Miele, L., Magnus, T., Poosala, S., Granger, D. N., & Mattson, M. P. (2006). Gamma secretase-mediated Notch signaling worsens brain damage and functional outcome in ischemic stroke. *Nature Medicine*, 12(6), 621–623. <https://doi.org/10.1038/nm1403>
- Aruoma, O. I., & Halliwell, B. (1987). Action of hypochlorous acid on the antioxidant protective enzymes superoxide dismutase, catalase and glutathione peroxidase. *Biochemical Journal*, 248(3), 973–976. <https://doi.org/10.1042/bj2480973>
- Blankesteyn, W. M., Essers-Janssen, Y. P., Verluyten, M. J., Daemen, M. J., & Smits, J. F. (1997). A homologue of *Drosophila* tissue polarity gene frizzled is expressed in migrating myofibroblasts in the infarcted rat heart. *Nature Medicine*, 3(5), 541–544. <https://doi.org/10.1038/nm0597-541>
- Bode, A. M., Ma, W. Y., Surh, Y. J., & Dong, Z. (2001). Inhibition of epidermal growth factor-induced cell transformation and activator protein 1 activation by [6]-gingerol. *Cancer Research*, 61(3), 850–853.
- Cachofeiro, V., Goicochea, M., de Vinuesa, S. G., Oubina, P., Lahera, V., & Luno, J. (2008). Oxidative stress and inflammation, a link between chronic kidney disease and cardiovascular disease. *Kidney International Supplements*, 74(111), S4–9. <https://doi.org/10.1038/ki.2008.516>
- De, A. (2011). Wnt/Ca²⁺ signaling pathway: A brief overview. *Acta Biochimica Et Biophysica Sinica*, 43(10), 745–756. <https://doi.org/10.1093/abbs/gmr079>
- Del Rio, D., Stewart, A. J., & Pellegrini, N. (2005). A review of recent studies on malondialdehyde as toxic molecule and biological marker of oxidative stress. *Nutrition Metabolism Cardiovascular Diseases*, 15(4), 316–328. <https://doi.org/10.1016/j.numecd.2005.05.003>
- Eefting, F., Rensing, B., Wigman, J., Pannekoek, W. J., Liu, W. M., Cramer, M. J., Lips, D. J., & Doevendans, P. A. (2004). Role of apoptosis in reperfusion injury. *Cardiovascular Research*, 61(3), 414–426. <https://doi.org/10.1016/j.cardiores.2003.12.023>
- Eguchi, M., Liu, Y., Shin, E. J., & Sweeney, G. (2008). Leptin protects H9c2 rat cardiomyocytes from H₂O₂-induced apoptosis. *FEBS Journal*, 275(12), 3136–3144. <https://doi.org/10.1111/j.1742-4658.2008.06465.x>
- Gasser, R. N. (1988). The interdependence of hypertension, calcium overload, and coronary spasm in the development of myocardial infarction. *Angiology*, 39(8), 761–772. <https://doi.org/10.1177/000331978803900809>
- Ghareib, S. A., El-Bassossy, H. M., Elberry, A. A., Azhar, A., Watson, M. L., & Banjar, Z. M. (2015). 6-Gingerol alleviates exaggerated vasoconstriction in diabetic rat aorta through direct vasodilation and nitric oxide generation. *Drug Design Development and Therapy*, 9, 6019–6026. <https://doi.org/10.2147/DDDT.S94346>
- Giordano, F. J. (2005). Oxygen, oxidative stress, hypoxia, and heart failure. *Journal of Clinical Investigation*, 115(3), 500–508. <https://doi.org/10.1172/JCI24408>
- Grant, C. M., Perrone, G., & Dawes, I. W. (1998). Glutathione and catalase provide overlapping defenses for protection against hydrogen peroxide in the yeast *Saccharomyces cerevisiae*. *Biochemical and Biophysical Research Communication*, 253(3), 893–898. <https://doi.org/10.1006/bbrc.1998.9864>
- Han, X., Liu, P., Liu, M., Wei, Z., Fan, S., Wang, X., Sun, S., & Chu, L. (2020). [6]-Gingerol Ameliorates ISO-Induced Myocardial Fibrosis by Reducing Oxidative Stress, Inflammation, and Apoptosis through Inhibition of TLR4/MAPKs/NF-kappaB Pathway. *Molecular Nutrition & Food Research*, 64(13), e2000003. <https://doi.org/10.1002/mnfr.202000003>
- Han, X., Zhang, Y., Liang, Y., Zhang, J., Li, M., Zhao, Z., Zhang, X., Xue, Y., Zhang, Y., Xiao, J., & Chu, L. (2019). 6-Gingerol, an active pungent component of ginger, inhibits L-type Ca²⁺ current, contractility, and Ca²⁺ transients in isolated rat ventricular myocytes. *Food Science & Nutrition*, 7(4), 1344–1352. <https://doi.org/10.1002/fsn3.968>
- Haniadka, R., Rajeev, A. G., Palatty, P. L., Arora, R., & Baliga, M. S. (2012). *Zingiber officinale* (ginger) as an anti-emetic in cancer chemotherapy: A review. *Journal of Alternative and Complementary Medicine*, 18(5), 440–444. <https://doi.org/10.1089/acm.2010.0737>
- Herlitz, J., Dellborg, M., Karlsson, T., Evander, M. H., Berger, A., & Luepker, R. (2008). Epidemiology of acute myocardial infarction with the emphasis on patients who did not reach the coronary care unit and non-AMI admissions. *International Journal of Cardiology*, 128(3), 342–349. <https://doi.org/10.1016/j.ijcard.2007.06.018>
- Hescheler, J., Meyer, R., Plant, S., Krautwurst, D., Rosenthal, W., & Schultz, G. (1991). Morphological, biochemical, and electrophysiological characterization of a clonal cell (H9c2) line from rat heart. *Circulation Research*, 69(6), 1476–1486. <https://doi.org/10.1161/01.res.69.6.1476>
- Hess, M. L., & Manson, N. H. (1984). Molecular oxygen: Friend and foe. The role of the oxygen free radical system in the calcium paradox, the oxygen paradox and ischemia/reperfusion injury. *Journal of Molecular & Cellular Cardiology*, 16(11), 969–985. [https://doi.org/10.1016/S0022-2828\(84\)80011-5](https://doi.org/10.1016/S0022-2828(84)80011-5)
- Hoekstra, K. A., Godin, D. V., Kurtu, J., & Cheng, K. M. (2003). Effects of oxidant-induced injury on heme oxygenase and glutathione in

- cultured aortic endothelial cells from atherosclerosis-susceptible and-resistant Japanese quail. *Molecular and Cellular Biochemistry*, 254(1-2), 61–71. <https://doi.org/10.1023/a:1027381110640>
- Hu, X., Ma, R., Lu, J., Zhang, K., Xu, W., Jiang, H., & Da, Y. (2016). IL-23 Promotes Myocardial I/R Injury by Increasing the Inflammatory Responses and Oxidative Stress Reactions. *Cellular Physiology Biochemistry*, 38(6), 2163–2172. <https://doi.org/10.1159/000445572>
- Hurst, S., Hoek, J., & Sheu, S. S. (2017). Mitochondrial Ca²⁺ and regulation of the permeability transition pore. *Journal of Bioenergetics and Biomembranes*, 49(1), 27–47. <https://doi.org/10.1007/s10863-016-9672-x>
- Jennings, R. B. (2013). Historical perspective on the pathology of myocardial ischemia/reperfusion injury. *Circulation Research*, 113(4), 428–438. <https://doi.org/10.1161/CIRCRESAHA.113.300987>
- Jian, J., Xuan, F., Qin, F., & Huang, R. (2016). The Antioxidant, anti-inflammatory and anti-apoptotic activities of the bauhinia championii flavone are connected with protection against myocardial ischemia/reperfusion injury. *Cellular Physiology Biochemistry*, 38(4), 1365–1375. <https://doi.org/10.1159/000443080>
- Jung, J. Y., Mo, H. C., Yang, K. H., Jeong, Y. J., Yoo, H. G., Choi, N. K., Oh, W. M., Oh, H. K., Kim, S. H., Lee, J. H., Kim, H. J., & Kim, W. J. (2007). Inhibition by epigallocatechin gallate of CoCl₂-induced apoptosis in rat PC12 cells. *Life Sciences*, 80(15), 1355–1363. <https://doi.org/10.1016/j.lfs.2006.11.033>
- Katiyar, S. K., Agarwal, R., & Mukhtar, H. (1996). Inhibition of tumor promotion in SENCAR mouse skin by ethanol extract of Zingiber officinale rhizome. *Cancer Research*, 56(5), 1023–1030. <https://doi.org/10.1007/s002620050271>
- Kroemer, G. (1999). Mitochondrial control of apoptosis: An overview. *Biochemical Society Symposia*, 66, 1–15. <https://doi.org/10.1042/bss0660001>
- Kühl, M., Sheldahl, L. C., Park, M., Miller, J. R., & Moon, R. T. (2000). The Wnt/Ca²⁺ pathway: A new vertebrate Wnt signaling pathway takes shape. *Trends in Genetics*, 16(7), 279–283. [https://doi.org/10.1016/S0168-9525\(00\)02028-X](https://doi.org/10.1016/S0168-9525(00)02028-X)
- Li, D., Williams, V., Liu, L., Chen, H., Sawamura, T., Antakli, T., & Mehta, J. L. (2002). LOX-1 inhibition in myocardial ischemia-reperfusion injury: Modulation of MMP-1 and inflammation. *American Journal of Physiology. Heart and Circulatory Physiology*, 283(5), H1795–1801. <https://doi.org/10.1152/ajpheart.00382.2002>
- Li, Y. Y., Xiao, L., Qiu, L. Y., Yan, Y. F., Wang, H., Duan, G. L., Liao, Z. P., & Chen, H. P. (2017). Sasanquasaponin-induced cardioprotection involves inhibition of mPTP opening via attenuating intracellular chloride accumulation. *Fitoterapia*, 116, 1–9. <https://doi.org/10.1016/j.fitote.2016.11.003>
- Madungwe, N. B., Zilberstein, N. F., Feng, Y., & Bopassa, J. C. (2016). Critical role of mitochondrial ROS is dependent on their site of production on the electron transport chain in ischemic heart. *American Journal of Cardiovascular Disease*, 6(3), 93–108.
- Maier, L. S., Christiane, S., Wolfgang, S., Kazutomo, M., Ulrich, S., & Burkert, P. (2000). Gingerol, isoproterenol and ouabain normalize impaired post-rest behavior but not force-frequency relation in failing human myocardium. *Cardiovascular Research*, 45(4), 913–924. [https://doi.org/10.1016/S0008-6363\(99\)00387-9](https://doi.org/10.1016/S0008-6363(99)00387-9)
- Minghetti, P., Sosa, S., Cilirzo, F., Casiraghi, A., Alberti, E., Tubaro, A., Loggia, R. D., & Montanari, L. (2007). Evaluation of the topical anti-inflammatory activity of ginger dry extracts from solutions and plasters. *Planta Medica*, 73(15), 1525–1530. <https://doi.org/10.1055/s-2007-993741>
- Moorjani, N., Westaby, S., Narula, J., Catarino, P. A., Brittin, R., Kemp, T. J., Narula, N., & Sugden, P. H. (2009). Effects of left ventricular volume overload on mitochondrial and death-receptor-mediated apoptotic pathways in the transition to heart failure. *American Journal of Cardiology*, 103(9), 1261–1268. <https://doi.org/10.1016/j.amjcard.2009.01.013>
- Muders, F., Neubauer, S., Luchner, A., Fredersdorf, S., Ickenstein, G., Riegger, G. A., Horn, M., & Elsner, D. (2001). Alterations in myocardial creatinine kinase (CK) and lactate dehydrogenase (LDH) isoenzyme-distribution in a model of left ventricular dysfunction. *European Journal of Heart Failure*, 3(1), 1–5. [https://doi.org/10.1016/s1388-9842\(00\)00085-4](https://doi.org/10.1016/s1388-9842(00)00085-4)
- Najib, K., Boateng, S., Sangodkar, S., Mahmood, S., Whitney, H., Wang, C. E., Racs, P., & Sanborn, T. A. (2015). Incidence and characteristics of patients presenting with acute myocardial infarction and non-obstructive coronary artery disease. *Catheterization and Cardiovascular Interventions*, 86(Suppl 1), S23–27. <https://doi.org/10.1002/ccd.26043>
- Namekata, I., Ohhara, M., Hirota, Y., Fukumoto, M., Kawanishi, T., Takahara, A., & Tanaka, H. (2008). SERCA activators, ellagic acid and gingerol, ameliorate diabetes mellitus-induced diastolic dysfunction in isolated murine ventricular myocardia. *Journal of Molecular and Cellular Cardiology*, <https://doi.org/10.1016/j.yjmcc.2008.09.701>
- Scarabelli, T. M., Stephanou, A., Pasini, E., Comini, L., Raddino, R., Knight, R. A., & Latchman, D. S. (2002). Different signaling pathways induce apoptosis in endothelial cells and cardiac myocytes during ischemia/reperfusion injury. *Circulation Research*, 90(6), 745–748. <https://doi.org/10.1161/01.res.0000015224.07870.9a>
- Shukla, Y., & Singh, M. (2007). Cancer preventive properties of ginger: A brief review. *Food and Chemical Toxicology*, 45(5), 683–690. <https://doi.org/10.1016/j.fct.2006.11.002>
- Slusarski, D. C., Corces, V. G., & Moon, R. T. (1997). Interaction of Wnt and a Frizzled homologue triggers G-protein-linked phosphatidylinositol signalling. *Nature*, 390(6658), 410–413. <https://doi.org/10.1038/37138>
- Slusarski, D. C., Yang-Snyder, J., Busa, W. B., & Moon, R. T. (1997). Modulation of embryonic intracellular Ca²⁺ signaling by Wnt-5A. *Development Biology*, 182(1), 114–120. <https://doi.org/10.1006/dbio.1996.8463>
- Tani, M. (1990). Mechanisms of Ca²⁺ overload in reperfused ischemic myocardium. *Annual Review of Physiology*, 52, 543–559. <https://doi.org/10.1146/annurev.ph.52.030190.002551>
- Turer, A. T., & Hill, J. A. (2010). Pathogenesis of myocardial ischemia-reperfusion injury and rationale for therapy. *American Journal of Cardiology*, 106(3), 360–368. <https://doi.org/10.1016/j.amjcard.2010.03.032>
- Wang, Y., Zhang, Z., Wang, X., Qi, D., Qu, A., & Wang, G. (2017). Amelioration of ethanol-induced hepatitis by magnesium isoglycyrrhizinate through inhibition of neutrophil cell infiltration and oxidative damage. *Mediators of Inflammation*, 2017, 3526903. <https://doi.org/10.1155/2017/3526903>
- Weiss, J. N., Korge, P., Honda, H. M., & Ping, P. (2003). Role of the mitochondrial permeability transition in myocardial disease. *Circulation Research*, 93(4), 292–301. <https://doi.org/10.1161/01.RES.0000087542.26971.D4>
- Whelan, R. S., Kaplinskiy, V., & Kitsis, R. N. (2010). Cell death in the pathogenesis of heart disease: Mechanisms and significance. *Annual Review of Physiology*, 72, 19–44. <https://doi.org/10.1146/annurev.physiol.010908.163111>
- Xiao, L., Lan, A., Mo, L., Xu, W., Jiang, N., Hu, F., Feng, J., & Zhang, C. (2012). Hydrogen sulfide protects PC12 cells against reactive oxygen species and extracellular signal-regulated kinase 1/2-mediated downregulation of glutamate transporter-1 expression induced by chemical hypoxia. *International Journal of Molecular Medicine*, 30(5), 1126–1132. <https://doi.org/10.3892/ijmm.2012.1090>
- Xie, Y., He, Y., Cai, Z., Cai, J., Xi, M., Zhang, Y., & Xi, J. (2016). Tauroursodeoxycholic acid inhibits endoplasmic reticulum stress, blocks mitochondrial permeability transition pore opening, and

- suppresses reperfusion injury through GSK-3 α in cardiac H9c2 cells. *American Journal of Translational Research*, 8(11), 4586–4597.
- Yellon, D. M., & Hausenloy, D. J. (1997). Myocardial reperfusion injury. *New England Journal of Medicine*, 4(11), 1121–1135. <https://doi.org/10.1056/NEJMra071667>
- Zhou, S. S., He, F., Chen, A. H., Hao, P. Y., & Song, X. D. (2012). Suppression of rat Frizzled-2 attenuates hypoxia/reoxygenation-induced Ca²⁺ accumulation in rat H9c2 cells. *Experimental Cell Research*, 318(13), 1480–1491. <https://doi.org/10.1016/j.yexcr.2012.03.030>
- Zhu, A., Wei, X., Zhang, Y., You, T., Yao, S., Yuan, S., Xu, H., Li, F., & Mao, W. (2017). Propofol Provides cardiac protection by suppressing the proteasome degradation of caveolin-3 in ischemic/reperfused rat hearts. *Journal of Cardiovascular Pharmacology*, 69(3), 170–177. <https://doi.org/10.1097/FJC.0000000000000454>
- Zhu, J., Huang, J., Dai, D., Wang, X., Gao, J., Han, W., & Zhang, R. (2019). Recombinant human interleukin-1 receptor antagonist treatment protects rats from myocardial ischemia-reperfusion injury. *Biomedicine & Pharmacotherapy*, 111, 1–5. <https://doi.org/10.1016/j.biopha.2018.12.031>

How to cite this article: Zheng B, Qi J, Liu P, et al. 10-Gingerol alleviates hypoxia/reoxygenation-induced cardiomyocyte injury through inhibition of the Wnt5a/Frizzled-2 pathway. *Food Sci Nutr*. 2021;9:3917–3931. <https://doi.org/10.1002/fsn3.2381>